New predictions for generalized spin polarizabilities from heavy baryon chiral perturbation theory

Chung-Wen Kao[1], Barbara Pasquini[2], and Marc Vanderhaeghen[3]
[1]*Department of Physics, North Carolina State University, Raleigh, NC27695-8202,USA*
[2] *Dipartimento di Fisica Nucleare e Teorica, Università degli Studi di Pavia; INFN, Sezione di Pavia, Pavia, Italy, and ECT*, Villazzano (Trento), Italy and*
[3]*Thomas Jefferson National Accelerator Facility, Newport News, VA 23606,USA and Department of Physics, College of William and Mary, Williamsburg,VA 23187,USA*
(Dated: February 2, 2008)

We extract the next-to-next-to-leading order results for spin-flip generalized polarizabilities (GPs) of the nucleon from the spin-dependent amplitudes for virtual Compton scattering (VCS) at $\mathcal{O}(p^4)$ in heavy baryon chiral perturbation theory. At this order, no unknown low energy constants enter the theory, allowing us to make absolute predictions for all spin-flip GPs. Furthermore, by using constraint equations between the GPs due to nucleon crossing combined with charge conjugation symmetry of the VCS amplitudes, we get a next-to-next-to-next-to-leading order prediction for one of the GPs. We provide estimates for forthcoming double polarization experiments which allow to access these spin-flip GPs of the nucleon.

PACS numbers: 13.60.Fz, 12.39.Fe, 13.40.-f,14.20.Dh

I. INTRODUCTION

Over the past decade, the virtual Compton scattering (VCS) process on the nucleon, accessed through the $ep \to ep\gamma$ reaction, has become a powerful new tool to study the internal structure of the nucleon both at low and high energies (see [1] for a review). At low virtuality and energy, the outgoing real photon plays the role of an applied quasi-static electromagnetic field, and the VCS process measures the response of the nucleon to this applied field, which can be parametrized in nucleon structure quantities, termed generalized polarizabilities (GPs) [2]. In this case, the virtuality of the initial photon can be dialed so as to map out the spatial distribution of the electric polarization, the magnetization, or the spin densities of the nucleon [3]. Because the chiral dynamics plays a dominant role in this regime, at low virtuality, Heavy Baryon Chiral Perturbation Theory (HBChPT) provides a natural way to study the GPs of the nucleon.

The spin-dependent VCS amplitudes in HBChPT at order $\mathcal{O}(p^3)$ have been calculated in Refs. [4, 5]. The HBChPT calculation for the spin-dependent VCS amplitudes has recently been extended to $\mathcal{O}(p^4)$ in Ref. [6]. At this order, no unknown low-energy constants enter the calculations so that one can extract the next-to-leading order (NLO) results for the spin-flip GPs of the nucleon, without free parameters. In Ref. [6], it was possible to extract the next order corrections to three of the seven spin-flip GPs in HBChPT by identifying the terms linear in the final photon energy in a low-energy expansion (LEX) of the spin-dependent VCS amplitudes.

In this paper, we demonstrate that by performing higher order expansions of the VCS amplitude with respect to the final photon energy, i.e. by including the terms quadratic in the final photon energy, one can furthermore extract the NNLO results of three more spin-flip GPs and even make a N^3LO prediction for one particular GP. In this way we are able to obtain the next order corrections to all seven spin-flip GPs in HBChPT, without free parameters.

On the experimental side, the measurement of the VCS process became only possible in recent years, with the advent of high precision electron accelerator facilities, as these experiments involve precision measurements of small cross sections. At low photon energy and virtuality, first unpolarized VCS observables have been measured at the MAMI accelerator [7] at a virtuality $Q^2 = 0.33$ GeV^2, and recently at JLab [8] at higher virtualities, $1 < Q^2 < 2$ GeV^2, and data are under analysis at MIT-Bates [9]. All those experiments measure two combinations of GPs. To disentangle the four independent spin-flip GPs, requires to perform in addition double polarization experiments. In this paper, we show predictions for such double polarization asymmetries and demonstrate their sensitivity to the spin-flip GPs.

The outline of this paper is as follows. We start in Section II by reviewing how the virtual Compton scattering amplitude at low photon energies can be expanded in terms of GPs. We subsequently review the status of the HBChPT calculations for the spin-flip GPs. In Section III, we outline how we can extract four spin-flip GPs at next order in HBChPT by performing a quadratic expansion in the final photon energy. In Section IV, we compare our predictions for the four independent spin-flip GPs at next order in HBChPT with the leading order (non-zero) expressions. Furthermore, we demonstrate the sensitivity of double polarization asymmetries to the spin-flip GPs. Finally we give our conclusions in Section V. Technical details on crossing symmetry relations for the VCS amplitudes can be found in an Appendix.

II. VIRTUAL COMPTON SCATTERING AND GENERALIZED POLARIZABILITIES

We begin by specifying our notation for the VCS process:

$$\gamma^*(\varepsilon_1, q) + N(p_1) \to \gamma(\varepsilon_2, q') + N(p_2). \tag{1}$$

The VCS amplitudes are calculated in the *c.m.* frame and we choose the Coulomb gauge [6]. In the VCS process, the initial spacelike photon is characterized by its four momentum $q = (\omega, \vec{q})$, virtuality $Q^2 \equiv -q^2$, and polarization vector $\varepsilon_1 = (0, \vec{\varepsilon}_1)$. The outgoing real photon has four momentum $q' = (\omega' = |\vec{q'}|, \vec{q'})$ and polarization vector $\varepsilon_2 = (0, \vec{\varepsilon}_2)$. We define $\bar{q} \equiv |\vec{q}|$, and denote θ as the scattering angle between virtual and real photons, i.e., $\cos\theta = \hat{q} \cdot \hat{q}^{\,\prime}$. The polarization vector $\vec{\varepsilon}_1$ of the virtual photon can be decomposed into a longitudinal component $\vec{\varepsilon}_{1L} = (\vec{\varepsilon}_1 \cdot \hat{q})\hat{q}$ and a transverse component $\vec{\varepsilon}_{1T}$. For further use, we introduce the virtual photon energy in the limit $\omega' = 0$:

$$\begin{aligned} \omega_0 \equiv \omega(\omega' = 0, \bar{q}) &= M_N - \sqrt{M_N^2 + \bar{q}^2}, \\ &= -\bar{q}^2/(2M_N) + \mathcal{O}(1/M_N^3), \end{aligned} \tag{2}$$

with M_N the nucleon mass, and where the last line in Eq. (2) indicates the heavy baryon expansion.

The VCS amplitude $\mathcal{M}_{VCS}$ can be expressed in terms of twelve structure functions as [4] :

$$\begin{aligned} \mathcal{M}_{VCS} &= ie^2\chi_f^\dagger \Big\{ (\vec{\varepsilon}_2^{\,*} \cdot \vec{\varepsilon}_{1T})A_1 + (\vec{\varepsilon}_2^{\,*} \cdot \hat{q})(\vec{\varepsilon}_{1T} \cdot \hat{q}')A_2 + i\vec{\sigma} \cdot (\vec{\varepsilon}_2^{\,*} \times \vec{\varepsilon}_{1T})A_3 + i\vec{\sigma} \cdot (\hat{q}' \times \hat{q})(\vec{\varepsilon}_2^{\,*} \cdot \vec{\varepsilon}_{1T})A_4 \\ &+ i\vec{\sigma} \cdot (\vec{\varepsilon}_2^{\,*} \times \hat{q})(\vec{\varepsilon}_{1T} \cdot \hat{q}')A_5 + i\vec{\sigma} \cdot (\vec{\varepsilon}_2^{\,*} \times \hat{q}')(\vec{\varepsilon}_{1T} \cdot \hat{q}')A_6 - i\vec{\sigma} \cdot (\vec{\varepsilon}_{1T} \times \hat{q}')(\vec{\varepsilon}_2^{\,*} \cdot \hat{q})A_7 - i\vec{\sigma} \cdot (\vec{\varepsilon}_{1T} \times \hat{q})(\vec{\varepsilon}_2^{\,*} \cdot \hat{q})A_8 \\ &+ (\vec{\varepsilon}_{1L} \cdot \hat{q}) \Big[(\vec{\varepsilon}_2^{\,*} \cdot \hat{q})A_9 + i\vec{\sigma} \cdot (\hat{q}' \times \hat{q})(\vec{\varepsilon}_2^{\,*} \cdot \hat{q})A_{10} + i\vec{\sigma} \cdot (\vec{\varepsilon}_2^{\,*} \times \hat{q})A_{11} + i\vec{\sigma} \cdot (\vec{\varepsilon}_2^{\,*} \times \hat{q}')A_{12} \Big] \Big\} \chi_i \,. \end{aligned} \tag{3}$$

To extract the GPs, we first calculate the complete fourth order VCS amplitudes A_i in HBChPT, and subsequently separate the amplitudes in a Born part A_i^{Born}, and a non-Born part $\bar{A}_i$ as :

$$A_i(\omega', \bar{q}, \theta) = A_i^{Born}(\omega', \bar{q}, \theta) + \bar{A}_i(\omega', \bar{q}, \theta), \tag{4}$$

In the Born process, the virtual photon is absorbed on a nucleon and the intermediate state remains a nucleon. We calculate them, following the definition of Ref. [2], from direct and crossed Born diagrams with the electromagnetic vertex given by :

$$\Gamma^\mu(q^2) = F_1(q^2)\gamma^\mu + F_2(q^2) i\sigma^{\mu\nu} \frac{q_\nu}{2M_N}, \tag{5}$$

where $F_1 (F_2)$ are the nucleon Dirac (Pauli) form factors respectively. The non-Born terms contain the information on the internal structure of the nucleon. In particular, we are interested in this work in the response of the nucleon to an applied quasi-static electromagnetic dipole field. This is accessed by performing a low energy expansion (LEX), in the outgoing photon energy, of the non-Born VCS amplitudes, and by selecting the term which is linear in the outgoing photon energy, given by :

$$\left[\frac{\partial \bar{A}_i}{\partial \omega'}(\omega', \bar{q}, \theta) \right]_{\omega'=0} = \mathcal{S}_i(\bar{q}) + \mathcal{P}_i(\bar{q}) \cos\theta. \tag{6}$$

In Eq. (6), the nucleon structure quantities $\mathcal{S}_i$ and $\mathcal{P}_i$ can be expressed in terms of the GPs of the nucleon, as introduced in [2], which are functions of $\bar{q}$ and which are denoted by $P^{(\rho' L', \rho L)S}(\bar{q})$. In this notation, ρ (ρ') refers to the electric (E), magnetic (M) or longitudinal (L) nature of the initial (final) photon, L (L') represents the angular momentum of the initial (final) photon, and S differentiates between the spin-flip ($S = 1$) and non spin-flip ($S = 0$) character of the transition at the nucleon side. Restricting oneself to a dipole transition for the final photon (i.e. L' = 1), angular momentum and parity conservation leads to 3 scalar and 7 spin GPs [2]. The 7 spin GPs are obtained as [10] :

$$\begin{aligned} P^{(M1,L2)1} &= \frac{-2\sqrt{2}}{3\sqrt{3}} \frac{1}{\bar{q}\,\omega_0} \sqrt{\frac{M_N}{E_N}} \mathcal{S}_{10}, \quad P^{(L1,L1)1} = \frac{-2}{3} \frac{1}{\omega_0} \sqrt{\frac{M_N}{E_N}} \mathcal{S}_{11}, \quad P^{(M1,L0)1} = \frac{2}{\sqrt{3}} \frac{\bar{q}}{\omega_0} \sqrt{\frac{M_N}{E_N}} \left[\mathcal{S}_{12} - \frac{2}{3}\mathcal{S}_{10} \right], \\ P^{(L1,M2)1} &= -\frac{\sqrt{2}}{3\bar{q}^2} \sqrt{\frac{M_N}{E_N}} \mathcal{S}_8, \quad P^{(M1,M1)1} = \frac{2}{3\bar{q}} \sqrt{\frac{M_N}{E_N}} \left[\mathcal{S}_7 - \mathcal{S}_4 \right], \\ \hat{P}^{(M1,2)1} &= -\frac{4}{3\sqrt{10}\bar{q}^3} \sqrt{\frac{M_N}{E_N}} \left[\mathcal{S}_4 + \mathcal{S}_7 - \mathcal{S}_{10} \right], \quad \hat{P}^{(L1,1)1} = -\frac{2\sqrt{2}}{3\sqrt{3}\bar{q}^2} \sqrt{\frac{M_N}{E_N}} \left[\mathcal{S}_3 + \frac{1}{2}\mathcal{S}_8 - \mathcal{S}_{11} \right], \end{aligned} \tag{7}$$

where $E_N = \sqrt{M_N^2 + \bar{q}^2}$, and where the GPs denoted by $\hat{P}$ correspond with mixed electric and longitudinal multipoles, as introduced in [2]. It has been shown [10] that nucleon crossing combined with charge conjugation symmetry of the VCS amplitudes provides 3 constraints among the 7 spin GPs :

$$\mathcal{S}_4 = 0, \qquad \mathcal{S}_3 = \frac{\bar{q}}{\omega_0}\mathcal{S}_7, \qquad \mathcal{S}_{10} - \mathcal{S}_{12} = \frac{\bar{q}}{\omega_0}\mathcal{S}_{11}, \tag{8}$$

leaving 4 independent spin GPs. By expanding ω_0 as in (2), it is obvious that the relations (8) connect quantities of different order in the heavy baryon expansion. These constraints have been verified in HBChPT in Ref. [6].

By calculating the VCS amplitudes in HBChPT at $\mathcal{O}(p^3)$, one extracts from Eq. (7) the following expressions for the GPs at LO (see Ref. [5]) :

$$\begin{aligned}
\left[P^{(M1,L2)1}(\bar{q})\right]^{LO} &= \left[P^{(M1,L0)1}(\bar{q})\right]^{LO} = \left[\hat{P}^{(M1,2)1}(\bar{q})\right]^{LO} = 0, \\
\left[P^{(M1,M1)1}(\bar{q})\right]^{LO} &= \left[P^{(L1,L1)1}(\bar{q})\right]^{LO} = 0, \\
\left[P^{(L1,M2)1}(\bar{q})\right]^{LO} &= \frac{-g_A^2}{24\sqrt{2}\pi^2 F_\pi^2 \bar{q}^2}\left\{1 - \frac{4}{w\sqrt{w^2+4}}\sinh^{-1}\left(\frac{w}{2}\right)\right\}, \\
\left[\hat{P}^{(L1,1)1}(\bar{q})\right]^{LO} &= \frac{g_A^2}{24\sqrt{6}\pi^2 F_\pi^2 \bar{q}^2}\left\{3 - \frac{4w^2+12}{w\sqrt{w^2+4}}\sinh^{-1}\left(\frac{w}{2}\right)\right\},
\end{aligned} \tag{9}$$

where $w \equiv \bar{q}/m_\pi$, with m_π the pion mass. Furthermore, throughout this paper we use the values : $g_A = 1.267$, $F_\pi = 0.0924$ GeV, and $m_\pi = 0.14$ GeV.

The VCS amplitudes in HBChPT at $\mathcal{O}(p^4)$, yield the GPs at NLO, from Eq. (7) (see Ref. [6]) :

$$\begin{aligned}
\left[P^{(M1,L2)1}(\bar{q})\right]^{NLO} &= \frac{-g_A^2}{12\sqrt{6}\pi^2 F_\pi^2 \bar{q}^2}\left\{1 - \frac{4}{w\sqrt{w^2+4}}\sinh^{-1}\left(\frac{w}{2}\right)\right\}, \\
\left[P^{(M1,L0)1}(\bar{q})\right]^{NLO} &= \frac{g_A^2}{12\sqrt{3}\pi^2 F_\pi^2}\left\{2 - \frac{3w^2+8}{w\sqrt{w^2+4}}\sinh^{-1}\left(\frac{w}{2}\right)\right\}, \\
\left[P^{(M1,M1)1}(\bar{q})\right]^{NLO} &= \frac{g_A^2}{24\pi^2 F_\pi^2 M_N}\left\{1 - \frac{w^2+4}{w\sqrt{w^2+4}}\sinh^{-1}\left(\frac{w}{2}\right)\right\}, \\
\left[\hat{P}^{(M1,2)1}(\bar{q})\right]^{NLO} &= \frac{-g_A^2}{24\sqrt{10}\pi^2 F_\pi^2 M_N \bar{q}^2}\left\{3 - \frac{2w^2+12}{w\sqrt{w^2+4}}\sinh^{-1}\left(\frac{w}{2}\right)\right\}, \\
\left[P^{(L1,L1)1}(\bar{q})\right]^{NLO} &= 0, \\
\left[P^{(L1,M2)1}(\bar{q})\right]^{NLO} &= \frac{g_A^2}{96\sqrt{2}\pi F_\pi^2 \bar{q}^2}\cdot\frac{\bar{q}}{M_N} \\
&\times \left\{\frac{1}{2w} + \frac{2w^2+4}{w(w^2+4)} + (\frac{5}{4} - \frac{3}{w^2})\tan^{-1}\left(\frac{w}{2}\right) + \tau_3\left[\frac{1}{2w} + (\frac{1}{4} - \frac{1}{w^2})\tan^{-1}\left(\frac{w}{2}\right)\right]\right\}, \\
\left[\hat{P}^{(L1,1)1}(\bar{q})\right]^{NLO} &= \frac{-g_A^2}{96\sqrt{6}\pi F_\pi^2 \bar{q}^2}\cdot\frac{\bar{q}}{M_N} \\
&\times \left\{\frac{11}{2w} - \frac{2w^2+4}{w(w^2+4)} - (\frac{25}{4} + \frac{9}{w^2})\tan^{-1}\left(\frac{w}{2}\right) + \tau_3\left[\frac{3}{2w} - (\frac{5}{4} + \frac{3}{w^2})\tan^{-1}\left(\frac{w}{2}\right)\right]\right\}.
\end{aligned} \tag{10}$$

One can get more predictions by use of the crossing relations (8), which hold in general in a relativistic quantum field theory, and which were calculated in HBChPT to $\mathcal{O}(p^4)$ in Ref. [6]. By plugging in the fourth order amplitudes in (8), we can extract fifth order predictions from $\mathcal{S}_3^{(4)} = -2M_N/\bar{q}\,\mathcal{S}_7^{(5)}$, and $\mathcal{S}_{10}^{(4)} - \mathcal{S}_{12}^{(4)} = -2M_N/\bar{q}\,\mathcal{S}_{11}^{(5)}$. In this way, these relations allow us to extract two spin GPs at next-to-next-to-leading order (NNLO) :

$$\begin{aligned}
\left[P^{(M1,M1)1}(\bar{q})\right]^{NNLO} &= \frac{-g_A^2\bar{q}}{192\pi F_\pi^2 M_N^2}\left\{\frac{3}{w} - (\frac{5}{2} + \frac{6}{w^2})\tan^{-1}\left(\frac{w}{2}\right) + \tau_3\left[\frac{1}{w} - (\frac{1}{2} + \frac{2}{w^2})\tan^{-1}\left(\frac{w}{2}\right)\right]\right\}, \\
\left[P^{(L1,L1)1}(\bar{q})\right]^{NNLO} &= \frac{g_A^2}{48\pi^2 F_\pi^2 M_N}\left\{-1 + \frac{2w^2+4}{w\sqrt{w^2+4}}\sinh^{-1}\left(\frac{w}{2}\right)\right\}.
\end{aligned} \tag{11}$$

It is surprising that the third order calculation [5] was able to obtain some of these NLO and one NNLO results! Actually, the NLO results for $P^{(M1,L2)1}$ and $P^{(M1,L0)1}$ were obtained in Refs. [4, 5], by performing the LEX of the amplitudes $\bar{A}_i$ to second order in ω', and, by isolating two terms at order ω'^2 which depend on those spin GPs. Furthermore, they used the crossing relations (8) to obtain the NLO results for $P^{(M1,M1)1}$ and $\hat{P}^{(M1,2)1}$, as well as

the NNLO result for $P^{(L1,L1)1}$.

In the present work, we generalize this method and obtain the NNLO result for $P^{(M1,L2)1}$, $P^{(M1,L0)1}$, and $\hat{P}^{(M1,2)1}$, and even the N^3LO result for $P^{(L1,L1)1}$. The first step is to define the following quantities:

$$\left[\frac{\partial^2 \bar{A}_i(\omega',\bar{q},\theta)}{\partial\omega'^2}\right]_{\omega'=0} = 2\alpha_i(\bar{q}) + 2\beta_i(\bar{q})\cos\theta + 2\gamma_i(\bar{q})\cos^2\theta. \tag{12}$$

Our goal is to express α_i, β_i and γ_i in terms of GPs. To achieve this goal, one needs to start from the covariant virtual Compton scattering tensor. The VCS amplitudes are obtained as the contraction of the VCS tensor $M_{\mu\nu}$ with the polarization vectors of the photons, evaluated between the nucleon spinors in the initial and the final states,

$$\mathcal{M}_{VCS} = -ie^2\bar{u}(p_1)\sum_{i=1}^{12}\varepsilon_{1\mu}\varepsilon^*_{2\nu}\rho_i^{\mu\nu} f_i(q^2, q\cdot q', q'\cdot P)u(p_2), \tag{13}$$

where $P = p_1 + p_2$, f_i are the VCS amplitudes, and $\rho_i^{\mu\nu}$ are the gauge-invariant independent tensor structures for VCS, as given by [10]. The key point of our method is to connect the covariant amplitudes f_i and the *c.m.* amplitudes A_i defined in Eq. (3). Subsequently, we will perform a low energy expansion of the amplitudes A_i and sort out the relations between f_i and the α_i, β_i and γ_i defined through Eq. (12). In addition, the GPs can also be expressed in terms of the covariant amplitudes f_i. Comparing both results will enable us to express the higher order coefficients of the LEX in terms of GPs. The advantage of working with the covariant Compton tensors is that symmetry properties due to photon crossing as well as nucleon crossing combined with charge conjugation, as derived in Ref. [10] and detailed in the Appendix, are immediately manifest.

III. CALCULATION OF GENERALIZED POLARIZABILITIES AT NNLO AND N^{3}LO IN HBCHPT

To extract the GPs at NNLO, we start by connecting both sets of VCS amplitudes A_i and f_i of Eqs. (3) and (13). To this goal, one has to expand $\varepsilon_{1\mu}\varepsilon^*_{2\nu}\rho_i^{\mu\nu}$ in Eq. (13) in ω' in the *c.m.* frame and also expand the non-Born parts of the amplitudes f_i in ω':

$$f_i^{non-Born} = \mathring{f}_i(\bar{q}) + \omega'\cdot[g_i(\bar{q}) + h_i(\bar{q})\cos\theta] + \mathcal{O}(\omega'^2). \tag{14}$$

For the new predictions of three NNLO GPs and one N^{3}LO GP which we will derive, we only need the amplitudes A_{10}, A_{11} and A_{12}. The expressions for these amplitudes including terms up to order ω'^2 can be found, after some algebra, as [20] :

$$\begin{aligned}
\bar{A}_{10} &= \omega'\left[2\omega_0\bar{q}\mathring{f}_4 - \frac{\omega_0^3}{2\bar{q}}\mathring{f}_5 - \frac{\omega_0\bar{q}}{2}\mathring{f}_7 - \frac{2\omega_0^2}{\bar{q}}\mathring{f}_{10} - 2\omega_0\bar{q}\mathring{f}_{11} - \frac{M_N\omega_0^3}{\bar{q}}\mathring{f}_{12}\right]\\
&+ \omega'^2\left[2\omega_0\bar{q}g_4 - \frac{\omega_0^3}{2\bar{q}}g_5 - \frac{\omega_0\bar{q}}{2}g_7 - \frac{2\omega_0^2}{\bar{q}}g_{10} - 2\omega_0\bar{q}g_{11} - \frac{M_N\omega_0^3}{\bar{q}}g_{12}\right]\\
&+ \omega'^2\cos\theta\left[2\omega_0\bar{q}h_4 - \frac{\omega_0^3}{2\bar{q}}h_5 - \frac{\omega_0\bar{q}}{2}h_7 - \frac{2\omega_0^2}{\bar{q}}h_{10} - 2\omega_0\bar{q}h_{11} - \frac{M_N\omega_0^3}{\bar{q}}h_{12}\right]\\
&+ \omega'^2[-\frac{\omega_0^2}{2M_N\bar{q}}\mathring{f}_1 + \omega_0\bar{q}\mathring{f}_2 + \left(2\bar{q} + \frac{\omega_0\bar{q}}{M_N}\right)\mathring{f}_4 + \left(-\frac{\omega_0^3}{4M_N\bar{q}} - \frac{\omega_0^2}{\bar{q}}\right)\mathring{f}_5 + \left(-\frac{4M_N\omega_0^2}{\bar{q}} + 2\omega_0^2\cos\theta\right)\mathring{f}_6 + \left(-\frac{\omega_0\bar{q}}{4M_N} - \frac{\bar{q}}{2}\right)\mathring{f}_7\\
&- \frac{\omega_0^2 M_N}{\bar{q}}\mathring{f}_8 + \omega_0\bar{q}\mathring{f}_9 + \frac{\bar{q}}{M_N}\mathring{f}_{10} + \left(-2\bar{q} - \frac{\omega_0\bar{q}}{M_N} - \frac{4\omega_0^2}{\bar{q}}\right)\mathring{f}_{11} + \left(-\frac{3\omega_0^3}{2\bar{q}} + \frac{\omega_0\bar{q}}{2}\right)\mathring{f}_{12}] + \mathcal{O}(\omega'^3),
\end{aligned} \tag{15}$$

$$\begin{aligned}
\bar{A}_{11} &= \omega'[(2\bar{q}^2 - 2\omega_0\bar{q}\cos\theta)\mathring{f}_4 + \left(-\frac{\omega_0^2}{2} + \frac{\omega_0^3}{2\bar{q}}\cos\theta\right)\mathring{f}_5 + \left(-\frac{\omega_0^2}{2} + \frac{\omega_0\bar{q}}{2}\cos\theta\right)\mathring{f}_7 + \left(-2\omega_0 + \frac{2\omega_0^2}{\bar{q}}\cos\theta\right)\mathring{f}_{10}\\
&+ \left(-2\omega_0^2 + 2\omega_0\bar{q}\cos\theta\right)\mathring{f}_{11} + \left(-2M_N\omega_0^2 + \frac{M_N\omega_0^3}{\bar{q}}\cos\theta\right)\mathring{f}_{12}]\\
&+ \omega'^2[\left(2\bar{q}^2 - 2\omega_0\bar{q}\cos\theta\right)g_4 + \left(-\frac{\omega_0^2}{2} + \frac{\omega_0^3}{2\bar{q}}\cos\theta\right)g_5 + \left(-\frac{\omega_0^2}{2} + \frac{\omega_0\bar{q}}{2}\cos\theta\right)g_7 + \left(-2\omega_0 + \frac{2\omega_0^2}{\bar{q}}\cos\theta\right)g_{10}\\
&+ \left(-2\omega_0^2 + 2\omega_0\bar{q}\cos\theta\right)g_{11} + \left(-2M_N\omega_0^2 + \frac{M_N\omega_0^3}{\bar{q}}\cos\theta\right)g_{12}]\\
&+ \omega'^2\cos\theta[\left(2\bar{q}^2 - 2\omega_0\bar{q}\cos\theta\right)h_4 + \left(-\frac{\omega_0^2}{2} + \frac{\omega_0^3}{2\bar{q}}\cos\theta\right)h_5 + \left(-\frac{\omega_0^2}{2} + \frac{\omega_0\bar{q}}{2}\cos\theta\right)h_7 + \left(-2\omega_0 + \frac{2\omega_0^2}{\bar{q}}\cos\theta\right)h_{10}
\end{aligned}$$

$$
\begin{aligned}
&+ \ (-2\omega_0^2 + 2\omega_0\bar{q}\cos\theta)h_{11} + \left(-2M_N\omega_0^2 + \frac{M_N\omega_0^3}{\bar{q}}\cos\theta\right)h_{12}] \\
&+ \ \omega'^2[-(4M_N + 2\bar{q}\cos\theta)\mathring{f}_4 - \left(\omega_0 - \frac{\omega_0^2}{\bar{q}}\cos\theta\right)\mathring{f}_5 + \left(-2\omega_0^2(1+\cos^2\theta) + \frac{2\omega_0}{\bar{q}}\cos\theta(\omega_0^2+\bar{q}^2)\right)\mathring{f}_6 \\
&+ \ \left(-\frac{\omega_0}{2} - \frac{M_N\omega_0}{\bar{q}}\cos\theta\right)\mathring{f}_7 + \left(\omega_0^2 - (\frac{M_N\omega_0^2}{\bar{q}} + \omega_0\bar{q})\cos\theta\right)\mathring{f}_8 + \left(\omega_0^2 - \omega_0\bar{q}\cos\theta\right)\mathring{f}_9 + \left(-2 + \frac{2\omega_0}{\bar{q}}\cos\theta\right)\mathring{f}_{10} \\
&+ \ \left(-6\omega_0 + (\frac{2\omega_0^2}{\bar{q}} + 2\bar{q})\cos\theta\right)\mathring{f}_{11} + \left(-\frac{3\omega_0^2}{2} - 2M_N\omega_0 + \frac{M_N\omega_0^2}{\bar{q}}\cos\theta\right)\mathring{f}_{12}] + \mathcal{O}(\omega'^3),
\end{aligned} \tag{16}
$$

$$
\begin{aligned}
\bar{A}_{12} \ = \ &\omega'\left[-\frac{M_N\omega_0^2}{\bar{q}}\mathring{f}_5 + \left(-\frac{2M_N^2\omega_0^2}{\bar{q}} + M_N\omega_0\bar{q}\right)\mathring{f}_{12}\right] \\
&+ \ \omega'^2\left[-\frac{M_N\omega_0^2}{\bar{q}}g_5 + \left(-\frac{2M_N^2\omega_0^2}{\bar{q}} + M_N\omega_0\bar{q}\right)g_{12}\right] + \omega'^2\cos\theta\left[-\frac{M_N\omega_0^2}{\bar{q}}h_5 + \left(-\frac{2M_N^2\omega_0^2}{\bar{q}} + M_N\omega_0\bar{q}\right)h_{12}\right] \\
&+ \ \omega'^2[\left(\frac{\omega_0\bar{q}}{M_N} - \frac{\omega_0^2}{M_N}\cos\theta\right)\mathring{f}_4 + \left(\frac{\bar{q}}{2} - \frac{3\omega_0^2}{2\bar{q}} - \frac{\omega_0\bar{q}}{4M_N} + \frac{\omega_0^2}{4M_N}\cos\theta\right)\mathring{f}_5 + \left(-\frac{4M_N\omega_0^2}{\bar{q}} + 4M_N\omega_0\cos\theta\right)\mathring{f}_6 \\
&+ \ \left(-\frac{\omega_0\bar{q}}{4M_N} + \frac{\bar{q}^2}{4M_N}\cos\theta\right)\mathring{f}_7 - \left(\frac{\omega_0^3}{2\bar{q}} + \frac{\omega_0\bar{q}}{2} - \omega_0^2\cos\theta\right)\mathring{f}_8 + \bar{q}(-\omega_0 + \bar{q}\cos\theta)\mathring{f}_9 + \left(\frac{\omega_0^2}{M_N\bar{q}} - \frac{\omega_0}{M_N}\cos\theta\right)\mathring{f}_{10} \\
&+ \ \left(-\frac{2\omega_0^2}{\bar{q}}(1 + \frac{\omega_0}{2M_N}) + (2\omega_0 + \frac{\omega_0^2}{M_N})\cos\theta\right)\mathring{f}_{11} + \left(2M_N\bar{q} - \frac{3M_N\omega_0^2}{\bar{q}} + \omega_0\bar{q} + \frac{\omega_0^2}{2}\cos\theta\right)\mathring{f}_{12}] \\
&+ \ \mathcal{O}(\omega'^3).
\end{aligned} \tag{17}
$$

We can simplify these expressions by using the crossing symmetry relations for the amplitudes f_i, as given in the Appendix, which lead to $\mathring{f}_4 = \mathring{f}_8 = \mathring{f}_{10} = 0$. It is now straightforward to read off from Eqs. (15 - 17) the coefficients $\mathcal{S}_i$ of Eq. (6), which appear in the LEX of the *c.m.* amplitudes $\bar{A}_i$, and express them as combinations of the $\mathring{f}_i$:

$$
\begin{aligned}
\mathcal{S}_{10} \ &= \ \left[-\frac{\omega_0^3}{2\bar{q}}\mathring{f}_5 - \frac{\omega_0\bar{q}}{2}\mathring{f}_7 - 2\omega_0\bar{q}\mathring{f}_{11} - \frac{M_N\omega_0^3}{\bar{q}}\mathring{f}_{12}\right], \\
\mathcal{S}_{11} \ &= \ \left[-\frac{\omega_0^2}{2}\mathring{f}_5 - \frac{\omega_0^2}{2}\mathring{f}_7 - 2\omega_0^2\mathring{f}_{11} - 2M_N\omega_0^2\mathring{f}_{12}\right], \\
\mathcal{S}_{12} \ &= \ \left[-\frac{M_N\omega_0^2}{\bar{q}}\mathring{f}_5 + \left(-\frac{2M_N^2\omega_0^2}{\bar{q}} + M_N\omega_0\bar{q}\right)\mathring{f}_{12}\right].
\end{aligned} \tag{18}
$$

By applying the defining relations of Eq. (7) for the GPs, one then obtains :

$$
\begin{aligned}
P^{(M1,L2)1}(\bar{q}) \ &= \ \frac{2\sqrt{2}}{3\sqrt{3}}\sqrt{\frac{E_N+M_N}{2E_N}}\left[\frac{\omega_0^2}{2\bar{q}^2}\mathring{f}_5 + \frac{1}{2}\mathring{f}_7 + 2\mathring{f}_{11} + \frac{M_N\omega_0^2}{\bar{q}^2}\mathring{f}_{12}\right], \\
P^{(M1,L0)1}(\bar{q}) \ &= \ \frac{2}{\sqrt{3}}\sqrt{\frac{E_N+M_N}{2E_N}}\left[\left(\frac{1}{3}\omega_0^2 - M_N\omega_0\right)\mathring{f}_5 + \frac{1}{3}\bar{q}^2\mathring{f}_7 + \frac{4}{3}\bar{q}^2\mathring{f}_{11} + \left(M_N\bar{q}^2 - 2M_N^2\omega_0 + \frac{2}{3}M_N\omega_0^2\right)\mathring{f}_{12}\right], \\
P^{(L1,L1)1}(\bar{q}) \ &= \ -\frac{2}{3}\sqrt{\frac{E_N+M_N}{2E_N}}\left[-\frac{\omega_0}{2}\mathring{f}_5 - \frac{\omega_0}{2}\mathring{f}_7 - 2\omega_0\mathring{f}_{11} - 2M_N\omega_0\mathring{f}_{12}\right].
\end{aligned} \tag{19}
$$

In general, the coefficients of order ω'^2 are combinations of $\mathring{f}$, g_i and h_i. On the other hand, the dipole GPs defined through Eq. (7) are all combinations of $\mathring{f}$. Actually g_i and h_i are related to higher order polarizabilities ($L' > 1$), and they can be defined in a similar way as in Ref. [2]. We leave the study of such higher order GPs to a future work and concentrate in this work on new predictions for dipole ($L' = 1$) GPs.

To compare with the amplitudes obtained from HBChPT, it is necessary to make the heavy baryon expansions on Eqs. (15 - 17). Note that not only ω_0 has to be expanded in $\bar{q}/M_N$ as in Eq. (2), but also $\mathring{f}_i$, g_i and h_i. Denoting any quantity proportional to $(1/M_N)^n$ by a superscript (n), we can express $\mathring{f}_i$ as :

$$
\mathring{f}_i = \mathring{f}_i^{(0)} + \mathring{f}_i^{(1)} + \mathcal{O}(1/M_N^2), \ i = 1,5,6,7,9,11. \tag{20}
$$

The amplitude f_{12} as well as the combination $2f_6 + f_9$ start with a contribution at $n = 1$ otherwise the amplitudes $\bar{A}_8$ and $\bar{A}_{12}$ would start at $n = -1$, which is obviously impossible. Also f_2 starts at $n = 1$ (otherwise $\bar{A}_9$ would also

start at $n = -1$), so that we can write :

$$\mathring{f}_i = \mathring{f}_i^{(1)} + \mathcal{O}(1/M_N^2),\ i = 2, 12. \tag{21}$$

The coefficients in the heavy baryon expansion are furthermore constrained by the crossing symmetry relations for the amplitudes f_i (for details, see the Appendix). We can then separate the leading and subleading terms in the heavy baryon expansion for the amplitudes $\bar{A}_{10}, \bar{A}_{11}$, and $\bar{A}_{12}$ as :

$$\begin{aligned}
\bar{A}_{10}^{LO} &= \omega'^2 \left[-\frac{\bar{q}}{2} \mathring{f}_7^{(0)} - 2\bar{q} \mathring{f}_{11}^{(0)} \right], \\
\bar{A}_{11}^{LO} &= \omega'^2 [2\bar{q}^2 g_4^{(0)}] + \omega'^2 \cos\theta \left[\frac{\bar{q}}{2} \mathring{f}_7^{(0)} + 2\bar{q} \mathring{f}_{11}^{(0)} \right], \\
\bar{A}_{12}^{LO} &= \omega'^2 \left[\frac{\bar{q}}{2} \mathring{f}_5^{(0)} + 2M_N \bar{q} \mathring{f}_{12}^{(1)} \right] + \omega'^2 \cos\theta [-2\bar{q}^2 \mathring{f}_6^{(0)} + \bar{q}^2 \mathring{f}_9^{(0)}], \\
\bar{A}_{10}^{NLO} &= \omega'^2 \left[-\frac{\bar{q}}{2} \mathring{f}_7^{(1)} - 2\bar{q} \mathring{f}_{11}^{(1)} \right] + \frac{1}{M_N} \omega' \left[\frac{\bar{q}^3}{4} \mathring{f}_7^{(0)} + \bar{q}^3 \mathring{f}_{11}^{(0)} \right] + \frac{1}{M_N} \omega'^2 [-\bar{q}^3 g_4^{(0)}] + \frac{1}{M_N} \omega'^2 \cos\theta \left[\frac{\bar{q}^3}{4} h_7^{(0)} + \bar{q}^3 h_{11}^{(0)} \right], \\
\bar{A}_{11}^{NLO} &= \omega'^2 [\bar{q}^2 \mathring{f}_{12}^{(1)} + 2\bar{q}^2 g_4^{(1)}] + \omega'^2 \cos\theta \left[\frac{\bar{q}}{2} \mathring{f}_7^{(1)} + 2\bar{q} \mathring{f}_{11}^{(1)} \right] \\
&+ \frac{1}{M_N} \omega' \cos\theta \left[-\frac{\bar{q}^3}{4} \mathring{f}_7^{(0)} - \bar{q}^3 \mathring{f}_{11}^{(0)} \right] + \frac{1}{M_N} \omega'^2 \left[\frac{\bar{q}^2}{2} \mathring{f}_5^{(0)} + \frac{\bar{q}^2}{4} \mathring{f}_7^{(0)} + 3\bar{q}^2 \mathring{f}_{11}^{(0)} + \bar{q}^2 g_{10}^{(0)} \right] \\
&+ \frac{1}{M_N} \omega'^2 \cos\theta \left[-\bar{q}^3 \mathring{f}_6^{(0)} + \frac{\bar{q}^3}{2} \mathring{f}_9^{(0)} + 2\bar{q}^3 g_4^{(0)} \right] + \frac{1}{M_N} \omega'^2 \cos^2\theta \left[\frac{-\bar{q}^3}{4} h_7^{(0)} - \bar{q}^3 h_{11}^{(0)} \right], \\
\bar{A}_{12}^{NLO} &= \omega'^2 \left[\frac{\bar{q}}{2} \mathring{f}_5^{(1)} + 2M_N \bar{q} \mathring{f}_{12}^{(2)} \right] + \frac{1}{M_N} \omega' \left[-\frac{\bar{q}^3}{4} \mathring{f}_5^{(0)} - M_N \bar{q}^3 \mathring{f}_{12}^{(1)} \right] + \frac{1}{M_N} \omega'^2 \left[-\bar{q}^3 \mathring{f}_6^{(0)} + \frac{\bar{q}^3}{2} \mathring{f}_9^{(0)} \right] \\
&+ \frac{1}{M_N} \omega'^2 \cos\theta \left[-2M_N \bar{q}^2 \mathring{f}_6^{(1)} + M_N \bar{q}^2 \mathring{f}_9^{(1)} + \frac{\bar{q}^2}{4} \mathring{f}_7^{(0)} - \bar{q}^2 \mathring{f}_{11}^{(0)} - \frac{\bar{q}^3}{4} h_5^{(0)} - M_N \bar{q}^3 h_{12}^{(1)} \right].
\end{aligned} \tag{22}$$

From Eq. (22) one can now identify the coefficients α_i, β_i and γ_i appearing in the LEX of Eq. (12) as follows :

$$\begin{aligned}
\alpha_{10}^{LO} &= -\frac{\bar{q}}{2} \mathring{f}_7^{(0)} - 2\bar{q} \mathring{f}_{11}^{(0)}, \quad \alpha_{10}^{NLO} = -\frac{\bar{q}}{2} \mathring{f}_7^{(1)} - 2\bar{q} \mathring{f}_{11}^{(1)} + \frac{1}{M_N} [-\bar{q}^3 g_4^{(0)}], \\
\beta_{10}^{LO} &= 0, \quad \beta_{10}^{NLO} = \frac{1}{M_N} \left[\frac{\bar{q}^3}{4} h_7^{(0)} + \bar{q}^3 h_{11}^{(0)} \right], \quad \gamma_{10}^{LO} = 0, \quad \gamma_{10}^{NLO} = 0, \\
\alpha_{11}^{LO} &= 2\bar{q}^2 g_4^{(0)}, \quad \alpha_{11}^{NLO} = \bar{q}^2 \mathring{f}_{12}^{(1)} + 2\bar{q}^2 g_4^{(1)} + \frac{1}{M_N} \left[\frac{\bar{q}^2}{2} \mathring{f}_5^{(0)} + \frac{\bar{q}^2}{4} \mathring{f}_7^{(0)} + 3\bar{q}^2 \mathring{f}_{11}^{(0)} + \bar{q}^2 g_{10}^{(0)} \right], \\
\beta_{11}^{LO} &= \frac{\bar{q}}{2} \mathring{f}_7^{(0)} + 2\bar{q} \mathring{f}_{11}^{(0)}, \quad \beta_{11}^{NLO} = \frac{\bar{q}}{2} \mathring{f}_7^{(1)} + 2\bar{q} \mathring{f}_{11}^{(1)} + \frac{1}{M_N} \left[-\bar{q}^3 \mathring{f}_6^{(0)} + \frac{\bar{q}^3}{2} \mathring{f}_9^{(0)} + 2\bar{q}^3 g_4^{(0)} \right], \\
\gamma_{11}^{LO} &= 0, \quad \gamma_{11}^{NLO} = \frac{1}{M_N} \left[\frac{-\bar{q}^3}{4} h_7^{(0)} - \bar{q}^3 h_{11}^{(0)} \right], \\
\alpha_{12}^{LO} &= \frac{\bar{q}}{2} \mathring{f}_5^{(0)} + 2M_N \bar{q} \mathring{f}_{12}^{(1)}, \quad \alpha_{12}^{NLO} = \frac{\bar{q}}{2} \mathring{f}_5^{(1)} + 2M_N \bar{q} \mathring{f}_{12}^{(2)} - \frac{\bar{q}^3}{M_N} \mathring{f}_6^{(0)} + \frac{\bar{q}^3}{2M_N} \mathring{f}_9^{(0)}, \\
\beta_{12}^{LO} &= [-2\bar{q}^2 \mathring{f}_6^{(0)} + \bar{q}^2 \mathring{f}_9^{(0)}] \quad \beta_{12}^{NLO} = \frac{1}{M_N} \left[-2M_N \bar{q}^2 \mathring{f}_6^{(1)} + M_N \bar{q}^2 \mathring{f}_9^{(1)} + \frac{\bar{q}^2}{4} \mathring{f}_7^{(0)} - \bar{q}^2 \mathring{f}_{11}^{(0)} - \frac{\bar{q}^3}{4} h_5^{(0)} - M_N \bar{q}^3 h_{12}^{(1)} \right], \\
\gamma_{12}^{LO} &= 0, \quad \gamma_{12}^{NLO} = 0.
\end{aligned} \tag{23}$$

The GPs of Eq. (19) can now be expressed in terms of the above LEX coefficients. The power counting of the GPs needs some word of explanation though. From HBChPT, the leading order amplitudes $\mathcal{S}_i^{(3)} \sim \mathcal{O}(1)$ and $\mathcal{S}_i^{(4)} \sim \mathcal{O}(1/M_N)$. Because ω_0 is a quantity of order $\mathcal{O}(1/M_N)$, one remarks from Eq. (7) that the three GPs $P^{(M1,L2)1}$, $P^{(L1,L1)1}$ and $P^{(M1,L0)1}$ should start at $\mathcal{O}(M_N)$. Actually $\mathcal{S}_{10}^{(3)} = \mathcal{S}_{11}^{(3)} = \mathcal{S}_{12}^{(3)} = 0$, and consequently these three GPs are non-zero only at NLO :

$$\left[P^{(M1,L2)1}(\bar{q}) \right]^{NLO} = \frac{2\sqrt{2}}{3\sqrt{3}} \left[\frac{1}{2} \mathring{f}_7^{(0)} + 2\mathring{f}_{11}^{(0)} \right] = -\frac{2\sqrt{2}}{3\sqrt{3}} \left[\frac{1}{\bar{q}} \alpha_{10}^{LO} \right],$$

$$
\begin{aligned}
\left[P^{(M1,L0)1}(\bar{q})\right]^{NLO} &= \frac{2}{\sqrt{3}}\left[\frac{\bar{q}^2}{2}\mathring{f}_5^{(0)} + \frac{1}{3}\bar{q}^2\mathring{f}_7^{(0)} + \frac{4}{3}\bar{q}^2\mathring{f}_{11}^{(0)} + 2M_N\bar{q}^2\mathring{f}_{12}^{(1)}\right] = \frac{2}{\sqrt{3}}\left[\bar{q}\alpha_{12}^{LO} - \frac{2}{3}\bar{q}\alpha_{10}^{LO}\right], \\
\left[P^{(M1,L2)1}(\bar{q})\right]^{NNLO} &= \frac{2\sqrt{2}}{3\sqrt{3}}\left[\frac{1}{2}\mathring{f}_7^{(1)} + 2\mathring{f}_{11}^{(1)}\right] = \frac{2\sqrt{2}}{3\sqrt{3}}\left[-\frac{1}{\bar{q}}\alpha_{10}^{NLO} - \frac{1}{2M_N}\alpha_{11}^{LO}\right], \\
\left[P^{(M1,L0)1}(\bar{q})\right]^{NNLO} &= \frac{2}{\sqrt{3}}\left[\frac{\bar{q}^2}{2}\mathring{f}_5^{(1)} + \frac{1}{3}\bar{q}^2\mathring{f}_7^{(1)} + \frac{4}{3}\bar{q}^2\mathring{f}_{11}^{(1)} + 2M_N\bar{q}^2\mathring{f}_{12}^{(2)}\right] \\
&= \frac{2}{\sqrt{3}}\left[\bar{q}\alpha_{12}^{NLO} - \frac{\bar{q}^2}{2M_N}\beta_{12}^{LO} - \frac{2}{3}\bar{q}\alpha_{10}^{NLO} - \frac{1}{3}\frac{\bar{q}^2}{M_N}\alpha_{11}^{LO}\right]. \qquad (24)
\end{aligned}
$$

To evaluate the GPs $P^{(M1,L2)1}$ and $P^{(M1,L0)1}$ at NNLO, requires the knowledge of the VCS amplitudes at $\mathcal{O}(p^5)$ in HBChPT through the coefficients α_{10}^{NLO} and α_{12}^{NLO}. In general, the amplitudes at $\mathcal{O}(p^5)$ in HBChPT contain two parts. The first one consists of two-loop diagrams and one-loop diagrams with one vertex from the third-order Lagrangian $\mathcal{L}_{\pi N}^{(3)}$. The second one consists of one-loop diagrams with vertices from the heavy baryon expansion. The main difference between both contributions is that the former ones contain no $1/M_N$ factor whereas the latter ones contain a $1/M_N^2$ pre-factor. We will present here the results due to the one-loop diagrams with vertices from the heavy baryon expansion. Taking into account these contributions will precisely restore the symmetry property due to nucleon crossing combined with charge conjugation, which relates the VCS amplitudes at different orders in the heavy baryon expansion. The new analytic structures which one can expect to arise at $\mathcal{O}(p^5)$ due to two-loop effects have then to satisfy the crossing relations separately.

We find for α_{10}^{NLO} and α_{12}^{NLO} by explicit calculation in HBChPT the following results :

$$
\begin{aligned}
\alpha_{11}^{LO} &= 0, \quad \beta_{12}^{LO} = 0, \\
\alpha_{10}^{NLO} &= \frac{g_A^2}{64M_N\pi F_\pi^2}\left\{\left[\frac{-2}{w} + \frac{4-6w^2}{4w+w^3} - \frac{4}{3}\cdot\frac{6+15w^2+2w^4}{4w+w^3} + (12+\frac{6}{w^2})\tan^{-1}\left(\frac{w}{2}\right)\right]\right. \\
&+ \left.\frac{1}{2}[(1+\kappa_v)-(1+\kappa_s)\tau_3]\left[-\frac{8}{w} + \frac{w}{3} + (2+\frac{16}{w^2})\tan^{-1}\left(\frac{w}{2}\right)\right]\right\}, \\
\alpha_{12}^{NLO} &= \frac{g_A^2}{64M_N\pi F_\pi^2}\left\{\left[\frac{-7}{w} + \frac{2w}{3} + (2+\frac{14}{w^2})\tan^{-1}\left(\frac{w}{2}\right)\right]\right. \\
&+ \frac{1}{2}[1+\kappa_v]\left[\frac{-3}{w} + \frac{w}{6} + 3\,(\frac{1}{2}+\frac{2}{w^2})\tan^{-1}\left(\frac{w}{2}\right)\right] \\
&+ \left.\frac{1}{2}[(1+\kappa_s)\tau_3]\left[\frac{-1}{w} - \frac{w}{6} + (\frac{5}{2}+\frac{2}{w^2})\tan^{-1}\left(\frac{w}{2}\right)\right]\right\}, \qquad (25)
\end{aligned}
$$

where $\kappa_v = 3.70$ ($\kappa_s = -0.12$) are the nucleon isovector (isoscalar) anomalous magnetic moments respectively. Combining Eqs. (24) and (25), allows us to obtain the NNLO results for two GPs :

$$
\begin{aligned}
\left[P^{(M1,L0)1}(\bar{q})\right]^{NNLO} &= \frac{g_A^2\bar{q}}{96\sqrt{3}M_N\pi F_\pi^2}\left\{\left[\frac{-17}{w} + 2w - \frac{8-12w^2}{4w+w^3} + \frac{8}{3}\cdot\frac{6+15w^2+2w^4}{4w+w^3} + (-18+\frac{30}{w^2})\tan^{-1}\left(\frac{w}{2}\right)\right]\right. \\
&+ [1+\kappa_v]\left[\frac{7}{2w} - \frac{w}{12} + (\frac{1}{4}-\frac{7}{w^2})\tan^{-1}\left(\frac{w}{2}\right)\right] \\
&+ \left.[(1+\kappa_s)\tau_3]\left[-\frac{19}{2w} + \frac{w}{12} + (\frac{23}{4}+\frac{19}{w^2})\tan^{-1}\left(\frac{w}{2}\right)\right]\right\}, \qquad (26) \\
\left[P^{(M1,L2)1}(\bar{q})\right]^{NNLO} &= \frac{-g_A^2}{48\sqrt{6}M_N\pi F_\pi^2\bar{q}}\left\{\left[\frac{-2}{w} + \frac{4-6w^2}{4w+w^3} - \frac{4}{3}\cdot\frac{6+15w^2+2w^4}{4w+w^3} + (12+\frac{6}{w^2})\tan^{-1}\left(\frac{w}{2}\right)\right]\right. \\
&+ \left.[(1+\kappa_v)-(1+\kappa_s)\tau_3]\left[-\frac{4}{w} + \frac{w}{6} + (1+\frac{8}{w^2})\tan^{-1}\left(\frac{w}{2}\right)\right]\right\}. \qquad (27)
\end{aligned}
$$

A third NNLO prediction follows by applying the crossing symmetry constraint of Eq. (8), i.e. $\mathcal{S}_{10} - \mathcal{S}_{12} = \frac{\bar{q}}{\omega_0}\mathcal{S}_{11}$, which yields the relation between 3 spin GPs :

$$
3\frac{\bar{q}^2}{\omega_0}P^{(L1,L1)1} = \sqrt{3}P^{(M1,L0)1} + \sqrt{\frac{3}{2}}\bar{q}^2P^{(M1,L2)1}. \qquad (28)
$$

After the heavy baryon expansion, this becomes :

$$-6M_N\,[P^{(L1,L1)1}]^{N^3LO} = \sqrt{3}[P^{(M1,L0)1}]^{NNLO} + \sqrt{\frac{3}{2}}\bar{q}^2[P^{(M1,L2)1}]^{NNLO}, \tag{29}$$

from which we obtain :

$$\begin{aligned}\left[P^{(L1,L1)1}(\bar{q})\right]^{N^3LO} &= \frac{g_A^2\bar{q}}{576M_N^2\pi F_\pi^2}\left\{\left[\frac{15}{w} - 2w + 3\cdot\frac{4-6w^2}{4w+w^3} - 4\cdot\frac{6+15w^2+2w^4}{4w+w^3} + (30-\frac{24}{w^2})\tan^{-1}\left(\frac{w}{2}\right)\right]\right.\\ &+ [1+\kappa_v]\left[-\frac{15}{2w} + \frac{w}{4} + (\frac{3}{4}+\frac{15}{w^2})\tan^{-1}\left(\frac{w}{2}\right)\right]\\ &+ \left.[(1+\kappa_s)\tau_3]\left[+\frac{27}{2w} - \frac{w}{4} + (-\frac{27}{4}-\frac{27}{w^2})\tan^{-1}\left(\frac{w}{2}\right)\right]\right\}. \end{aligned}\tag{30}$$

Similarly, by applying the crossing symmetry constraint of Eq. (8), i.e. $\mathcal{S}_4 = 0$, which yields the relation between 3 spin GPs :

$$\sqrt{\frac{3}{2}}\omega_0 P^{(M1,L2)1}(\bar{q}) + P^{(M1,M1)1}(\bar{q}) + \sqrt{\frac{5}{2}}\bar{q}^2\hat{P}^{(M1,2)1} = 0, \tag{31}$$

one can get the NNLO result of $\hat{P}^{(M1,2)1}$:

$$\begin{aligned}\left[\hat{P}^{(M1,2)1}(\bar{q})\right]^{NNLO} &= \frac{-g_A^2}{96\sqrt{10}M_N^2\pi F_\pi^2\bar{q}}\left\{\left[\frac{-5}{w} + \frac{4-6w^2}{4w+w^3} - \frac{4}{3}\cdot\frac{6+15w^2+2w^4}{4w+w^3} + (\frac{29}{2}+\frac{12}{w^2})\tan^{-1}\left(\frac{w}{2}\right)\right]\right.\\ &+ [(1+\kappa_v)-(1+\kappa_s)\tau_3]\left[-\frac{4}{w} + \frac{w}{6} + (1+\frac{8}{w^2})\tan^{-1}\left(\frac{w}{2}\right)\right] + \tau_3\left.\left[-\frac{1}{w} + (\frac{1}{2}+\frac{2}{w^2})\tan^{-1}\left(\frac{w}{2}\right)\right]\right\}. \end{aligned}\tag{32}$$

At the real photon point ($\bar{q} = 0$), we can express the GP $P^{(M1,L2)1}(0)$ in terms of a sum of two spin polarizabilities ($\gamma_2 + \gamma_4$), introduced by Ragusa [11], as :

$$\gamma_2 + \gamma_4 = -\alpha_{em}\frac{3\sqrt{3}}{2\sqrt{2}}P^{(M1,L2)1}(0),$$

where $\alpha_{em} \equiv e^2/(4\pi) = 1/137$. The result of Eq. (27) then allows to extract the result for $\gamma_2 + \gamma_4$ at NLO as :

$$(\gamma_2+\gamma_4)^{NLO} = \frac{\alpha_{em}g_A^2}{384\pi F_\pi^2 m_\pi M_N}\left[-3 + 2(1+\kappa_v) - 2(1+\kappa_s)\tau_3\right], \tag{33}$$

which exactly reproduces the NLO calculations for $\gamma_2 + \gamma_4$ of Refs. [12, 13].

From our results, it is also worth noting that the crossing relations of Eq. (8) allow to classify the GPs into two groups :

$$\begin{aligned}\text{group 1} &= \left\{P^{(M1,L2)1}, P^{(M1,L0)1}, P^{(M1,M1)1}, \hat{P}^{(M1,2)1}\right\},\\ \text{group 2} &= \left\{P^{(L1,L1)1}, P^{(L1,M2)1}, \hat{P}^{(L1,1)1}\right\}.\end{aligned}$$

It is interesting to observe that their analytical forms alternate from one order to the next, as noticed already in Ref. [6]. At LO one has :

$$\text{group 1}: \frac{1}{\pi}\tan^{-1}\left(\frac{\bar{q}}{2m_\pi}\right); \quad \text{group 2}: \frac{1}{\pi^2}\sinh^{-1}\left(\frac{\bar{q}}{2m_\pi}\right).$$

At NLO, one has :

$$\text{group 1}: \frac{1}{\pi^2}\sinh^{-1}\left(\frac{\bar{q}}{2m_\pi}\right); \quad \text{group 2}: \frac{1}{\pi}\tan^{-1}\left(\frac{\bar{q}}{2m_\pi}\right).$$

At NNLO one again has the same analytical structure as at LO, etc. One therefore observes that the alternating analytical forms teach us how the crossing relations (8), connecting the GPs between two different orders in HBChPT, work. The same alternating analytical form were observed when comparing leading and next-to-leading order HBChPT results for the forward spin polarizabilities in Ref. [14].

IV. RESULTS AND DISCUSSION

The main result of this work are the new NNLO predictions of Eqs. (26, 27) and (32) for the spin GPs $P^{(M1,L0)1}$, $P^{(M1,L2)1}$, and $\hat{P}^{(M1,2)1}$, as well as the N^{3}LO prediction of Eq. (30) for the spin GP $P^{(L1,L1)1}$.

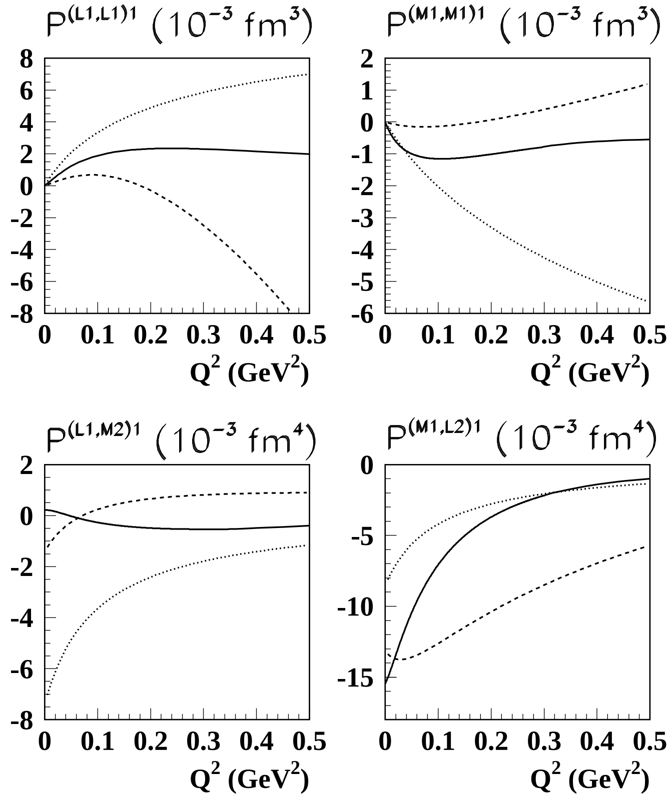

FIG. 1: Results for the spin GPs in HBChPT. For the GP $P^{(L1,M2)1}$, both the LO (dotted curve) and NLO (dashed curve) results are shown. For the GPs $P^{(M1,M1)1}$ and $P^{(M1,L2)1}$, both the NLO results (dotted curves) and the NNLO results (dashed curves) are shown. For the GP $P^{(L1,L1)1}$, the NNLO (dotted curve) and N^{3}LO (dashed curve) results are shown. For comparison, we also show the dispersive evaluation of Refs. [15, 16] (solid curves).

In Fig. 1, we compare these results for the GPs $P^{(M1,L2)1}$ and $P^{(L1,L1)1}$ with their lowest order non-zero expressions, and display as well the next order results for the GPs $P^{(L1,M2)1}$ and $P^{(M1,M1)1}$, which were calculated before in Ref. [6]. Note that the three remaining spin GPs of Eq. (7) can be expressed in terms of these four independent spin GPs by making use of the crossing symmetry relations of Eq. (8). By comparing the lowest order with next order results in HBChPT for each of the GPs, one observes large corrections at next order. We also compare these results in Fig. 1 with the phenomenological estimate of Refs. [15, 16] using dispersion relations. One sees that for the GPs $P^{(L1,M2)1}, P^{(M1,M1)1}$ and $P^{(L1,L1)1}$ the corrections to the leading order bring the HBChPT results towards the phenomenological estimates, though overshoots it for $P^{(L1,L1)1}$. For the GP $P^{(M1,L2)1}$, the sizeable large correction at the real photon point brings the HBChPT results close to the dispersive results but shows a much slower fall-off with Q^2 than the dispersive estimate. The comparison in Fig. 1 clearly indicates that a satisfactory description of spin GPs is still a challenging task. To completely disentangle the four spin GPs experimentally, requires four independent observables, which we discuss in the following.

It was shown in Ref. [2] that GPs can be accessed experimentally by measuring the $ep \to ep\gamma$ reaction and performing a low energy expansion in the outgoing photon energy ω'. In particular, the VCS unpolarized squared amplitude $\mathcal{M}^{\mathrm{exp}}$ takes on the form [2] :

$$\mathcal{M}^{\mathrm{exp}} = \frac{\mathcal{M}^{\mathrm{exp}}_{-2}}{\omega'^2} + \frac{\mathcal{M}^{\mathrm{exp}}_{-1}}{\omega'} + \mathcal{M}^{\mathrm{exp}}_0 + O(\omega') \,. \tag{34}$$

Due to the low energy theorem (LET), the threshold coefficients $\mathcal{M}^{\mathrm{exp}}_{-2}$ and $\mathcal{M}^{\mathrm{exp}}_{-1}$ are known [2], and are fully determined from the Bethe-Heitler + Born (BH + B) amplitudes. The information on the GPs is contained in $\mathcal{M}^{\mathrm{exp}}_0$,

which contains a part originating from the BH+B amplitudes and another one which is a linear combination of the GPs, with coefficients determined by the kinematics. The unpolarized observable $\mathcal{M}_0^{\rm exp}$ can be expressed in terms of three structure functions $P_{LL}(\bar{q})$, $P_{TT}(\bar{q})$, and $P_{LT}(\bar{q})$ as [2] :

$$\mathcal{M}_0^{\rm exp} - \mathcal{M}_0^{\rm BH+B} = 2K_2 \left\{ v_1 \left[\varepsilon P_{LL}(\bar{q}) - P_{TT}(\bar{q})\right] + \left(v_2 - \frac{\omega_0}{\bar{q}} v_3\right) \sqrt{2\varepsilon\,(1+\varepsilon)} P_{LT}(\bar{q}) \right\}, \tag{35}$$

where K_2 is a kinematical factor, ε is the virtual photon polarization (in the standard notation used in electron scattering), and v_1, v_2, v_3 are kinematical quantities depending on ε and $\bar{q}$ as well as on the *c.m.* polar and azimuthal angles ($\theta_{\gamma\gamma}$ and ϕ, respectively) of the produced real photon (for details see Ref. [1]). The three unpolarized observables of Eq. (35) can be expressed in terms of the independent GPs as [1, 2] :

$$P_{LL} \;=\; -2\sqrt{6}\, M_N\, G_E(Q^2)\, P^{(L1,L1)0}\,, \tag{36}$$

$$P_{TT} \;=\; -3\, G_M(Q^2)\, \frac{\bar{q}^2}{\omega_0} \left(P^{(M1,M1)1} \;-\; \sqrt{2}\, \omega_0\, P^{(L1,M2)1} \right), \tag{37}$$

$$P_{LT} \;=\; \sqrt{\frac{3}{2}}\, \frac{M_N\, \bar{q}}{Q}\, G_E(Q^2)\, P^{(M1,M1)0} \;+\; \frac{3}{2}\, \frac{Q\, \bar{q}}{\omega_0}\, G_M(Q^2)\, P^{(L1,L1)1}, \tag{38}$$

where $Q^2 \equiv \bar{q}^2 - \omega_0^2 = -2M_N\omega_0$, and $G_E(Q^2)$ and $G_M(Q^2)$ stand for the electric and magnetic nucleon form factors respectively. The spin independent GPs $P^{(L1,L1)0}$ and $P^{(M1,M1)0}$ are directly proportional to the electric and magnetic polarizabilities of the nucleon respectively. A Fourier transform of their $\bar{q}$-dependence allows us to map out the spatial distribution of the electric polarization and magnetization of the nucleon, as discussed in Ref. [3].

The first VCS experiment was performed at MAMI [7] and the response functions P_{LT} and P_{LL} - P_{TT}/ε were extracted at $Q^2 = 0.33$ GeV^2. Going to higher Q^2, the VCS process has also been measured at JLab and data have been obtained at $Q^2 = 1$ GeV^2 and $Q^2 = 1.9$ GeV^2 [8]. To unambiguously extract the spin-independent GPs from experiment, requires to separate P_{LL} from P_{TT}. This can be done by performing two unpolarized VCS experiments at a fixed value of $\bar{q}$ (or equivalently Q^2) and by varying ε (or equivalently the beam energy). Such experiments are planned at MAMI in the near future, making use of the beam energy upgrade. Besides extracting the electric GP $P^{(L1,L1)0}$, such an experiment will also allow for a measurement of the combination of the two spin GPs $P^{(M1,M1)1}$ and $P^{(L1,M2)1}$ of Eq. (37).

Until now, we discussed only unpolarized VCS observables. An unpolarized VCS experiment gives access to only three combinations of the six GPs, as given by Eqs. (36) - (38). It was shown in Ref. [17] that VCS double polarization observables with polarized lepton beam and polarized target (or recoil) nucleon, will allow us to measure three more combinations of spin-flip GPs. Therefore a measurement of unpolarized VCS observables (at different values of ε) and of three double-polarization observables will enable us to disentangle all six GPs. The VCS double polarization observables, which are denoted by $\Delta\mathcal{M}(h, i)$ for an electron of helicity h, are defined as the difference of the squared amplitudes for recoil (or target) proton spin orientation in the direction and opposite to the axis i ($i = x, y, z$), where the z-direction is chosen along the virtual photon momentum (see Ref. [17] for details). In a LEX, this polarized squared amplitude yields :

$$\Delta\mathcal{M}^{\rm exp} = \frac{\Delta\mathcal{M}_{-2}^{\rm exp}}{\omega'^2} + \frac{\Delta\mathcal{M}_{-1}^{\rm exp}}{\omega'} + \Delta\mathcal{M}_0^{\rm exp} + O(\omega')\,. \tag{39}$$

Analogously to the unpolarized squared amplitude of Eq. (34), the threshold coefficients $\Delta\mathcal{M}_{-2}^{\rm exp}$, $\Delta\mathcal{M}_{-1}^{\rm exp}$ are known due to the LET. It was found in Ref. [17] that the polarized squared amplitude $\Delta\mathcal{M}_0^{\rm exp}$ can be expressed in terms of three new structure functions $P_{LT}^{z}(\bar{q})$, $P_{LT}^{'z}(\bar{q})$, and $P_{LT}^{'\perp}(\bar{q})$. These new structure functions are related to the spin GPs as [1, 17] :

$$P_{LT}^{z} \;=\; \frac{3\, Q\, \bar{q}}{2\, \omega_0}\, G_M(Q^2)\, P^{(L1,L1)1} \;-\; \frac{3\, M_N\, \bar{q}}{Q}\, G_E(Q^2)\, P^{(M1,M1)1}, \tag{40}$$

$$P_{LT}^{'z} \;=\; -\frac{3}{2}\, Q\, G_M(Q^2)\, P^{(L1,L1)1} \;+\; \frac{3\, M_N\, \bar{q}^2}{Q\, \omega_0}\, G_E(Q^2)\, P^{(M1,M1)1}, \tag{41}$$

$$P_{LT}^{'\perp} \;=\; \frac{3\, \bar{q}\, Q}{2\, \omega_0}\, G_M(Q^2) \left(P^{(L1,L1)1} \;-\; \sqrt{\frac{3}{2}}\, \omega_0\, P^{(M1,L2)1} \right). \tag{42}$$

While P_{LT}^{z} and $P_{LT}^{'z}$ can be accessed by in-plane kinematics ($\phi = 0^{\rm o}$), the measurement of $P_{LT}^{'\perp}$ requires an out-of-plane experiment.

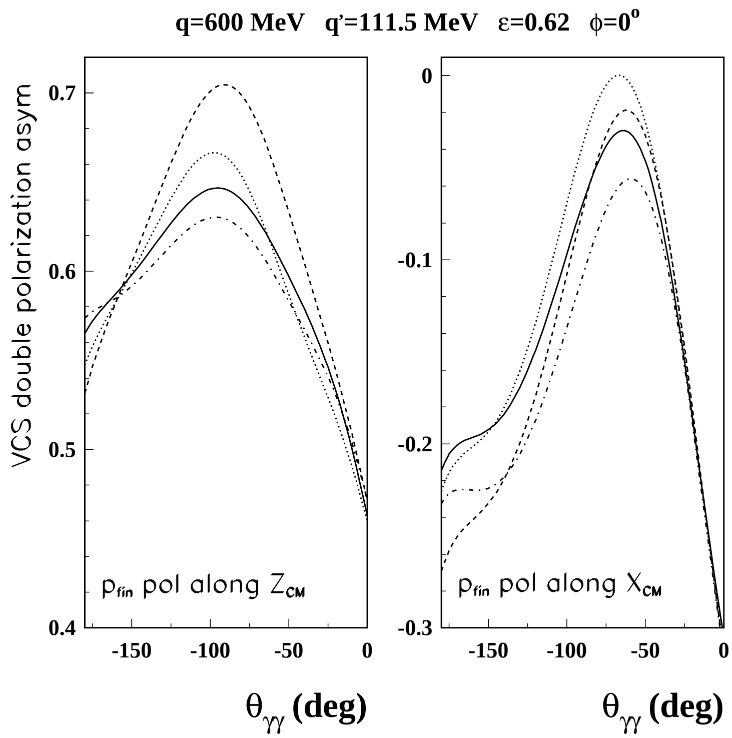

FIG. 2: VCS double-polarization asymmetry (polarized electron, recoil proton polarization along either the z- or x- directions in the *c.m.* frame) in MAMI kinematics as function of the photon scattering angle. The dashed-dotted curves correspond to the BH+B contribution. The dotted curves are the lowest order HBChPT predictions from Refs. [4, 5]. The dashed curves are obtained by including the next order HBChPT correction for all spin-flip GPs, as calculated in this work, while using the lowest order predictions for the spin-independent GPs. For comparison, we also show the results of a phenomenological dispersion relation calculation [16, 18] (solid curves).

In Fig. 2, we show the results for the double polarization observables, with polarized electron and by measuring the recoil proton polarization either along the virtual photon direction (z-direction) or parallel to the reaction plane and perpendicular to the virtual photon (x-direction). These asymmetries directly depend on the response functions of Eqs. (40)-(42). One sees from Fig. 2 that the double polarization asymmetries are quite large (due to a non-vanishing asymmetry for the BH + B mechanism). We furthermore compare in Fig. 2 the HBChPT predictions for the lowest order (non-vanishing) results for the spin GPs from Refs. [4, 5], with the next-order results for the spin GPs, as calculated in this work. For the spin independent GPs, which also enter in these asymmetries, we use in both cases the LO results, awaiting a NLO calculation for $P^{(L1,L1)0}$ and $P^{(M1,M1)0}$. One observes from Fig. 2 sizeable differences in the asymmetries between the leading order and next order HBChPT predictions for the spin GPs. For comparison, we also show in Fig. 2 the results of the DR calculation of Refs. [16, 18]. Due to the smaller spin GPs in the dispersion calculation, the relative effect on the asymmetries is smaller in the DR approach.

To quantify the relative effect on the asymmetries due to the spin GPs, we display in Fig. 3 the double polarization asymmetries with the well known Bethe-Heitler + Born contribution subtracted. Another contribution which is well known is the anomaly contribution (due to a t-channel π^0 pole) to the spin GPs, which is shown in Fig. 3 (lower panels). One furthermore sees from Fig. 3 (upper panels) that the effect of the spin GPs, excluding the anomaly contribution, on the double polarization asymmetries is of the order of 5 %. To distinguish between the different predictions, a double polarization VCS experiment is clearly called for. Although these double polarization observables are tough to measure, a first test experiment is already underway at MAMI [19].

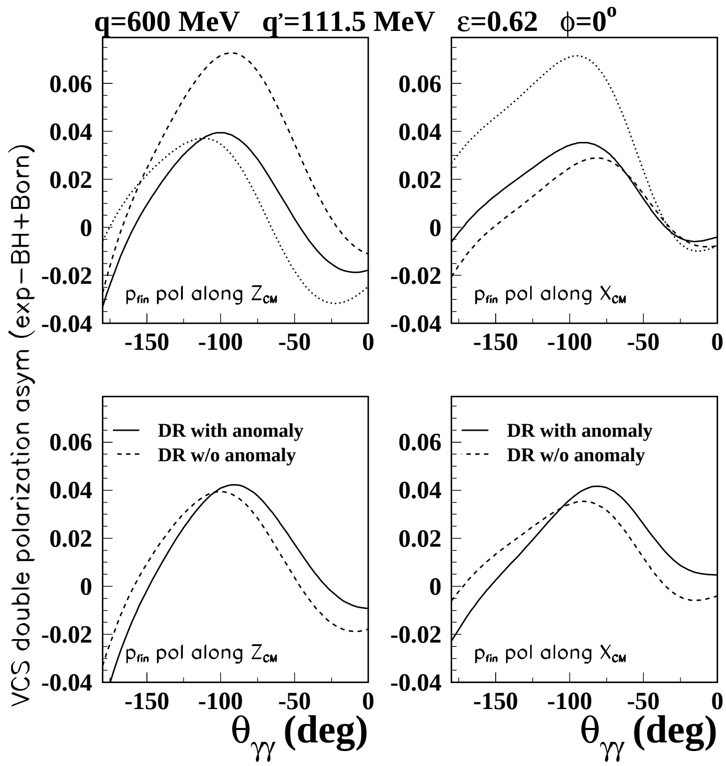

FIG. 3: Deviation of the double-polarization VCS asymmetry from the BH+Born result, calculated within the LEX formalism in MAMI kinematics as function of the photon scattering angle. Upper panels: lowest order HBChPT predictions from Refs. [4, 5] (dotted curves); results including the next order HBChPT corrections for the spin-flip GPs, as calculated in this work, and using the leading order predictions for the spin-independent GPs (dashed curves); dispersion relation results [16, 18] (solid curves). The effect of the anomaly contribution (i.e. t-channel π^0 pole) is neglected in all the three model-predictions. In the lower panels, a comparison is shown between the dispersive predictions without the anomaly contribution (dashed curves) and with the anomaly contribution (solid curves).

V. CONCLUSIONS

In this work, we calculated the spin-dependent VCS amplitude in HBChPT at $\mathcal{O}(p^4)$. In a low energy expansion of the outgoing photon energy, the spin-dependent VCS amplitude can be parametrized in terms of 7 generalized spin polarizabilities which characterize the response of the nucleon. Nucleon crossing symmetry combined with charge conjugation invariance leads to relations among these GPs, leaving four independent spin-flip GPs. We calculated all seven spin-flip GPs in HBChPT at $\mathcal{O}(p^4)$ and checked the three crossing symmetry relations to this order. At order $\mathcal{O}(p^4)$, no unknown low-energy constants enter the theory, allowing us to make absolute predictions for all seven spin-flip GPs to this order. Three of the spin-flip GPs at next order have been extracted before in Ref. [6] by identifying the term linear in the outgoing photon energy in the LEX of the spin-dependent VCS amplitudes. In the present work, we calculated within HBChPT at $\mathcal{O}(p^4)$ the quadratic terms in the outgoing photon energy, in which the dipole GPs also appear. From these quadratic terms, we were able to extract the remaining four spin-flip GPs at next order in HBChPT. A noteworthy feature of our results is that we provide analytical expressions for all spin-flip GPs at next order, analogously as has been done at lowest order in Ref. [5]. Another interesting feature arises from the crossing symmetry relations which connect the HBChPT amplitudes at different orders. As a result, our prediction for the GP $P^{(L1,L1)1}$ is formally a N^{3}LO result, and could only be obtained from a HBChPT calculation at $\mathcal{O}(p^5)$, if one were not to use the crossing relations.

Our predictions show sizeable corrections to the leading order (non-zero) results for the spin-flip GPs. The sign of these corrections is such as to move the leading order results in the direction of a phenomenological estimate of GPs based on dispersion relations. As the spin-flip GPs allow for absolute predictions at two successive orders in HBChPT without new low-energy constants entering, they may also be useful as a testing ground of chiral theories. It would

therefore be desirable to have direct experimental information on the spin-flip GPs to test the different predictions.

One combination of the four spin-flip GPs can be extracted by doing an unpolarized VCS experiment at a fixed value of Q^2 and by varying the beam energy. One can extract the other three spin-flip GPs through VCS double polarization observables with polarized lepton beam and polarized recoil nucleon. We gave predictions of these double polarization asymmetries for experimental conditions accessible at MAMI. We found that the relative effect on these asymmetries due to the spin-flip GPs is of the order of 5 %. Although the measurement of these asymmetries requires dedicated experiments, such a measurement would challenge the parameter-free chiral predictions at next order for the spin-flip GPs presented in this work.

Acknowledgments

This work was supported by the U.S. Department of Energy under contract DE-DF0-97ER41048 (C.W.K.), and contracts DE-FG02-04ER41302 (M.V.) and DE-AC05-84ER40150 (M.V.). The work of B.P. was supported by the Italian MIUR through the PRIN Theoretical Physics of the Nucleus and the Many-Body Systems.

APPENDIX A: CROSSING SYMMETRY PROPERTIES OF THE VCS AMPLITUDES IN THE COVARIANT BASIS

In this appendix, we study the properties of the amplitudes f_i under nucleon crossing combined with charge conjugation, which transforms $f_i(q^2, q \cdot q', q \cdot P)$ into $f_i(q^2, q \cdot q', -q \cdot P)$. First we expand the arguments of the amplitudes f_i as :

$$\begin{aligned}
f_i(q^2, q \cdot q', q \cdot P) &= \sum_{a,b,c} \mathcal{C}^i_{abc} \cdot (q^2)^a \cdot (q \cdot q')^b \cdot (q \cdot P)^c, \\
q^2 &= 2M_N\omega_0 + 2\omega_0 \cdot \omega' + (\frac{\omega_0}{M_N} + 1) \cdot \omega'^2 + \mathcal{O}(\omega'^3), \\
q \cdot q' &= 0 + (\omega_0 - \bar{q}\cos\theta) \cdot \omega' + 1 \cdot \omega'^2 + \mathcal{O}(\omega'^3), \\
q \cdot P &= 0 + (\frac{-\bar{q}^2}{\omega_0} + \bar{q}\cos\theta) \cdot \omega' + 1 \cdot \omega'^2 + \mathcal{O}(\omega'^3).
\end{aligned} \tag{A1}$$

Now we obtain :

$$\begin{aligned}
\mathring{f}_i &= \sum_{a=0}^{\infty} \mathcal{C}^i_{a00} (2M_N\omega_0)^a, \\
g_i &= \sum_{a=0}^{\infty} \mathcal{C}^i_{a10} (2M_N\omega_0)^a \omega_0 + \sum_{a=0}^{\infty} \mathcal{C}^i_{a01} (2M_N\omega_0)^a (2M_N - \omega_0) + \sum_{a=1}^{\infty} \mathcal{C}^i_{a00} \cdot a (2M_N\omega_0)^{a-1} \cdot 2\omega_0, \\
h_i &= \sum_{a=0}^{\infty} -\mathcal{C}^i_{a10} (2M_N\omega_0)^a \bar{q} + \sum_{a=0}^{\infty} \mathcal{C}^i_{a01} (2M_N\omega_0)^a \bar{q},
\end{aligned} \tag{A2}$$

where $\mathcal{C}^i_{abc}$ are the coefficients which start at $n = 0$, and $\mathcal{C}^i_{abc} \equiv \sum_{n=0}^{\infty} \frac{1}{M_N^n} \cdot \mathcal{C}^{i(n)}_{abc}$.

It was shown in Ref. [10] that nucleon crossing symmetry combined with charge conjugation leads to the following symmetry properties of the amplitudes f_i :

$$\begin{aligned}
f_i(q^2, q \cdot q', q \cdot P) &= f_i(q^2, q \cdot q', -q \cdot P), \quad i = 1, 2, 5, 6, 7, 9, 11, 12, \\
f_i(q^2, q \cdot q', q \cdot P) &= -f_i(q^2, q \cdot q', -q \cdot P), \quad i = 3, 4, 8, 10.
\end{aligned} \tag{A3}$$

Furthermore, photon crossing leads to the symmetry relations at the real photon point :

$$f_i(0, q \cdot q', q \cdot P) = 0\,, \quad i = 7, 9. \tag{A4}$$

From these symmetry relations, we obtain for the coefficients entering the expansion of Eq. (A1) :

$$\begin{aligned}
\mathcal{C}^i_{a01} &= 0, \quad i = 1, 2, 5, 6, 11, 12, \\
\mathcal{C}^i_{a10} &= \mathcal{C}^i_{a00} = 0, \quad i = 3, 4, 8, 10, \\
\mathcal{C}^i_{a01} &= \mathcal{C}^i_{010} = 0, \quad i = 7, 9.
\end{aligned} \tag{A5}$$

As a result, we obtain for the LEX of Eq. (14) :

$$\begin{aligned} g_i &= \sum_{a=0}^{\infty} \mathcal{C}^i_{a10}(2M_N\omega_0)^a\omega_0 + \sum_{a=1}^{\infty} \mathcal{C}^i_{a00}\cdot a(2M_N\omega_0)^{a-1}\cdot 2\omega_0, \\ h_i &= \sum_{a=0}^{\infty} -\mathcal{C}^i_{a10}(2M_N\omega_0)^a\bar{q}, \quad \text{for} \quad i=1,2,5,6,11,12, \end{aligned} \tag{A6}$$

furthermore

$$\begin{aligned} \mathring{f}_i &= 0,\ g_i = \sum_{a=0}^{\infty} \mathcal{C}^i_{a01}(2M_N\omega_0)^a(2M_N-\omega_0), \\ h_i &= \sum_{a=0}^{\infty} \mathcal{C}^i_{a01}(2M_N\omega_0)^a\bar{q}, \quad \text{for} \quad i=3,4,8,10, \end{aligned} \tag{A7}$$

and

$$\begin{aligned} g_i &= \sum_{a=1}^{\infty} \mathcal{C}^i_{a10}(2M_N\omega_0)^a\omega_0 + \sum_{a=1}^{\infty} \mathcal{C}^i_{a00}\cdot a(2M_N\omega_0)^{a-1}\cdot 2\omega_0, \\ h_i &= \sum_{a=1}^{\infty} -\mathcal{C}^i_{a10}(2M_N\omega_0)^a\bar{q}, \quad \text{for} \quad i=7,9. \end{aligned} \tag{A8}$$

The above results in turn yield relations for the coefficients in the heavy baryon expansion as in Eqs. (20,21). Since in the heavy baryon expansion, ω_0 is counted as $n=1$ and $2M_N\omega_0$ as $n=0$, we obtain :

$$g_1^{(0)} = g_2^{(0)} = g_5^{(0)} = g_6^{(0)} = g_7^{(0)} = g_9^{(0)} = g_{11}^{(0)} = g_{12}^{(0)} = 0. \tag{A9}$$

Moreover we know

$$2f_6^{(0)} + f_9^{(0)} = f_{12}^{(0)} = 0,$$

because otherwise the amplitudes $\bar{A}_8$ and $\bar{A}_{12}$ would start at $n=-1$ which is impossible. Therefore

$$2\mathring{f}_6^{(0)} + \mathring{f}_9^{(0)} = \mathring{f}_{12}^{(0)} = 0, \tag{A10}$$

and analogously

$$\begin{aligned} 2g_6^{(0)} + g_9^{(0)} &= g_{12}^{(0)} = 0, \\ 2h_6^{(0)} + h_9^{(0)} &= h_{12}^{(0)} = 0. \end{aligned} \tag{A11}$$

From $h_{12}^{(0)} = 0$ it follows that $C_{a10}^{12(n=0)} = 0$, and from $\mathring{f}_{12}^{(0)} = 0$ it follows that $C_{a00}^{12(n=0)} = 0$. Therefore we obtain $g_{12}^{(1)} = 0$. Similarly, one can show that :

$$\begin{aligned} &2g_6^{(1)} + g_9^{(1)} = 0, \\ &h_3^{(0)} = h_4^{(0)} = h_8^{(0)} = h_{10}^{(0)} = 0. \end{aligned} \tag{A12}$$

otherwise g_3, g_4, g_8, g_{10} will start at $n=-1$. Lastly, Eq. (A7) yields the relations :

$$h_i^{(1)} = g_i^{(0)} \cdot \frac{\bar{q}}{2M_N}, \quad \text{for} \quad i=3,4,8,10. \tag{A13}$$

---

[1] P.A.M. Guichon and M. Vanderhaeghen, Prog. Part. Nucl. Phys. **41**, 125 (1998).
[2] P.A.M. Guichon, G. Q. Liu and A. W Thomas, Nucl. Phys. **A 591**, 606 (1995).

[3] A.I. L'vov, S. Scherer, B. Pasquini, C. Unkmeir, and D. Drechsel, Phys. Rev. C **64**, 015203 (2001).
[4] T. R. Hemmert, B. R. Holstein, G. Knöchlein, and S. Scherer, Phys. Rev. Lett. **79**, 22 (1997); Phys. Rev. D **55**, 2630 (1997).
[5] T.R. Hemmert, B.R. Holstein, G. Knöchlein, and D. Drechsel, Phys. Rev. D **62**, 014013 (2000).
[6] C.-W. Kao and M. Vanderhaeghen, Phys. Rev. Lett. **89**, 272002 (2002).
[7] J. Roche *et al.*, Phys. Rev. Lett. **85**, 708 (2000).
[8] G. Laveissière *et al.* (The Jefferson Lab Hall A Collaboration), Phys. Rev. Lett. (2004) in press; hep-ph/0404243.
[9] R. Miskimen, spokesperson MIT-Bates Experiment, 97-03.
[10] D. Drechsel, G. Knöchlein, A.Yu Korchin, A. Metz, S. Scherer, Phys. Rev. C **57**, 941(1998);*ibid.* **58**, 1751(1998).
[11] S. Ragusa, Phys. Rev. D **47**, 3757 (1993); *ibid.* **49**, 3157 (1994).
[12] K.B. Vijaya Kumar, J.A. McGovern, and M.C. Birse, Phys. Lett. B **479**, 167 (2000).
[13] G.C. Gellas, T.R. Hemmert, and U.-G. Meißner, Phys. Rev. Lett. **85**, 14 (2000); *ibid.* **86**, 3205 (2001).
[14] C.-W. Kao, T. Spitzenberg, and M. Vanderhaeghen, Phys. Rev. D **67**, 016001 (2003).
[15] B. Pasquini, D. Drechsel, M. Gorchtein, A. Metz, and M. Vanderhaeghen, Phys. Rev. C **62**, 052201 (R) (2000).
[16] B. Pasquini, M. Gorchtein, D. Drechsel, A. Metz, and M. Vanderhaeghen, Eur. Phys. J. A **11**, 185 (2001).
[17] M. Vanderhaeghen, Phys. Lett. B **402**, 243 (1997).
[18] D. Drechsel, B. Pasquini, and M. Vanderhaeghen, Phys. Rep. **378**, 99 (2003).
[19] N. d'Hose, H. Merkel, spokespersons MAMI Experiment (2001).
[20] Note that we omit the global normalization factor $\sqrt{\frac{E_N+M_N}{2M_N}}$ on the *rhs* of Eqs. (15 - 17).